Amyloid-Like Fibrillogenesis through Supramolecular Helix-Mediated Self-Assembly of Tetrapeptides Containing Non-Coded α-Aminoisobutyric Acid (Aib) and 3-Aminobenzoic Acid (*m*-ABA)

by **Arpita Dutta**[a]), **Michael G. B. Drew**[b]), and **Animesh Pramanik***[a])

[a]) Department of Chemistry, University of Calcutta, 92 A. P. C. Road, Kolkata-700009, India (phone: +91-33-24841647; fax: +91-33-23519755; e-mail: animesh_in2001@yahoo.co.in)

[b]) School of Chemistry, The University of Reading, Whiteknights, Reading, RG66AD, UK

Single-crystal X-ray diffraction studies of two terminally protected tetrapeptides Boc-Ile-Aib-Val-*m*-ABA-OMe (**I**) and Boc-Ile-Aib-Phe-*m*-ABA-OMe (**II**) (Aib = α-aminoisobutyric acid; *m*-ABA = *meta*-aminobenzoic acid) reveal that they form continuous H-bonded helices through the association of double-bend (type III and I) building blocks. NMR Studies support the existence of the double-bend (type III and I) structures of the peptides in solution also. Field emission scanning electron-microscopic (FE-SEM) and high-resolution transmission electron-microscopic (HR-TEM) images of the peptides exhibit amyloid-like fibrils in the solid state. The Congo red-stained fibrils of peptide **I** and **II**, observed between crossed polarizers, show green-gold birefringence, a characteristic of amyloid fibrils.

Introduction. – Self-assembled supramolecular helices are present in many biologically important macromolecules such as collagen [1] and the tobacco mosaic virus coat protein [2]. It has been shown that helical self-assembly of amino acids can produce nanotubular [3] and nano-rod [4] structures. It is established that not only β-sheets but also helices have a significant role in amyloid-fibril formation where the α-helices are stacked along the fibril axis [5][6]. *Goldsbury et al.* have suggested that, for human amylin, α-helices may have a role in highly ordered self-aggregated amyloid plaque formation [7][8]. In the amyloidogenic peptide calcitonin, tape-like structures twist back upon themselves to afford hollow tube-like assemblies [9]. Although there are several examples of amyloid-like fibril formations through β-sheet-mediated self-assembly of small synthetic peptides in the literature [10–19], examples of amyloid-like fibrillogenesis through helix-mediated self-assembly of small synthetic peptides are limited [20][21]. Therefore, in this study, we were interested in designing small synthetic peptides that exhibit turns and have the potential to form supramolecular helical structures through molecular self-assembly, to gain more insights about fibrillogenesis.

In this context, we chose tetrapeptides Boc-Ile-Aib-Val-*m*-ABA-OMe (**I**) and Boc-Ile-Aib-Phe-*m*-ABA-OMe (**II**) (Aib = α-aminoisobutyric acid; *m*-ABA = *meta*-aminobenzoic acid) to examine the formation of supramolecular helices (*Fig. 1*). Generally, conformationally restricted Aib is a β-sheet breaker and highly helicogenic [22–30]. Therefore, tetrapeptides **I** and **II** with Aib at position 2 are expected to adopt turn structures which can act as building blocks for supramolecular helix formation through self-assembly. Aromatic π–π interactions are known to provide favorable

energetic contributions as well as order and directionality in the self-assembly of amyloid structures [31]. Therefore, incorporation of *m*-ABA, a substituted γ-aminobutyric acid with an all *trans*-extended configuration in **I** and **II**, and phenylalanine in **II** may help in self-assembly through aromatic $\pi-\pi$ interactions. Peptides were synthesized according to conventional solution-phase methodology, and their crystal-state structures were determined by X-ray diffraction analysis. Peptide conformations in the solution phase were probed by solvent-dependent NMR titrations and CD measurements. Field emission scanning electron microscopy (FE-SEM) and high-resolution transmission electron microscopy (HR-TEM) have been employed to examine the morphological properties of the peptides in the solid state.

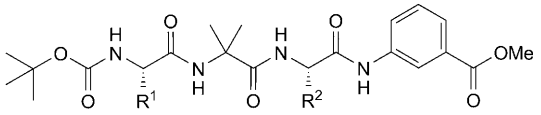

Fig. 1. *Structures of peptides* **I** *and* **II**

Results and Discussion. – *Peptide Conformations and Packing in Solid State.* Peptide **I** crystallizes with one molecule in the crystallographic asymmetric unit. The backbone torsion angles ($\phi$and ψ) at Ile and Aib are in the right-handed helical region (α_R) (*Table 1*). But, the ϕ and ψ values at Val ($-73.9(2)$ and $-5.8(2)^\circ$, resp.) deviate significantly from the ideal α_R region. *Fig. 2* shows that the tetrapeptide **I** adopts an overlapping double β-turn structure. The highly helicogenic Aib(2) induces two overlapping β-turn conformations in **I** stabilized by two intramolecular $4\rightarrow1$ H-bonds between NH of Val(3) and C=O of Boc (N(9)–H$\cdots$O(2)), and NH of *m*-ABA(4) and C=O of Ile(1) (N(12)–H$\cdots$O(5); *Table 2*). In the two overlapping β-turns, Ile(1)-Aib(2) occupies the corner position of the first β-turn of type III, and Aib(2)-Leu(3) occupies the corner position of the next β-turn of type I (*Fig. 2*). The residue Aib(2) simultaneously occupies the $i+2$ position of the first turn and the $i+1$ position for the succeeding turn.

The crystal structure of peptide **II** reveals two independent molecules **IIA** and **IIB** in the asymmetric unit that, while having different conformations, adopt 'diastereoisomeric' consecutive double β-turn structures (*Fig. 3*). The two overlapping β-turn conformations in **IIA** are stabilized by two intramolecular H-bonds between NH of Phe(3) and C=O of Boc (N(9A)–H$\cdots$O(2A)), and NH of *m*-ABA(4) and C=O of Ile(1) (N(12A)–H$\cdots$O(5A); *Table 2*). The residues Ile(1)-Aib(2) occupy the corner positions of the first β-turn of type III, and Aib(2)-Phe(3) occupies the corner positions of the next β-turn of type I (*Fig. 3*). The conformation of **IIA** is, therefore, similar to that found in **I** as is apparent from the torsion angles in *Table 1*. However, this is not the case for the conformation of **IIB** as, in spite of having L-amino acids along with achiral Aib and *m*-ABA, a 'diastereoisomeric' consecutive β-turn structure of type III′ is observed in **IIB**, where the backbone torsion angles (ϕ and ψ) are of opposite signs to those in **IIA** and thus belong to the left-handed helical region (α_L; *Table 1*). The residue Aib, which is a strongly helicogenic amino acid with practically no intrinsic preference

Table 1. *Selected Backbone Torsion Angles in Peptides* **I** *and* **II**

Residue	φ [°]	ψ [°]	ω [°]
Peptide **I**			
Ile(1)	– 64.0(2)	– 18.8(2)	– 172.2(1)
Aib(2)	– 49.1(2)	– 31.7(2)	179.0(1)
Val(3)	– 73.9(2)	– 5.8(2)	– 174.8(1)
Peptide **II**			
Molecule A			
Ile(1)	– 56.3(6)	– 37.8(6)	– 172.2(4)
Aib(2)	– 51.4(6)	– 32.0(6)	– 179.3(4)
Phe(3)	– 85.9(5)	– 10.1(6)	– 176.3(5)
Molecule B			
Ile(1)	45.3(6)	51.7(6)	173.2(4)
Aib(2)	55.0(7)	29.8(6)	174.7(4)
Phe(3)	60.1(6)	37.1(6)	179.4(4)

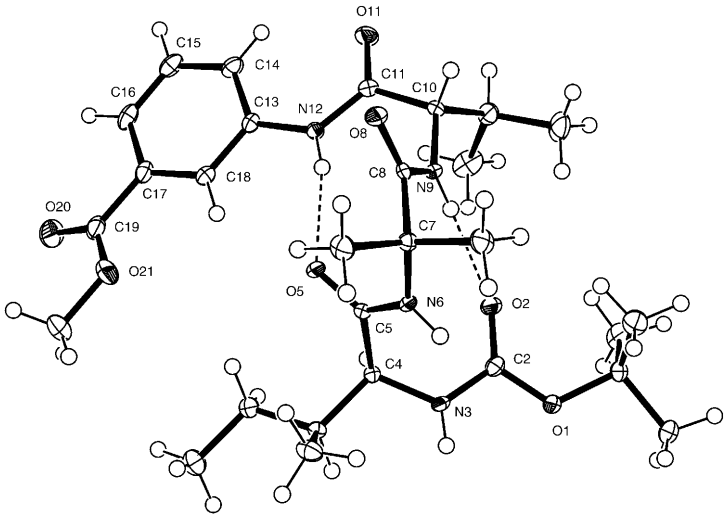

Fig. 2. *ORTEP Diagram of peptide* **I** *with ellipsoids at 50% probability* (H-bonds shown as dotted lines)

for helix handedness [32–34], induces this left-handed **IIB** conformation with some energy penalty. The conformational isomorphism of β-turns has biological implications, since interconversion between β-turn types have been observed in HIV protease [35]. It is noted that all the structures of **I** and **II** contain two intramolecular H-bonds, N(9)–H···O(2) and N(12)–H···O(5), which characterize the double-turn conformation.

The preorganized double β-turn building blocks of peptide **I** are stacked along the *c* axis through one intermolecular H-bond N(3)–H···O(8) between NH of Ile(1) and C=O of Aib(2) to form a supramolecular helical assembly (*Fig. 4* and *Table 2*). It is noteworthy that N(6)–H is not involved in any H-bond. Peptide **II** also undergoes self-

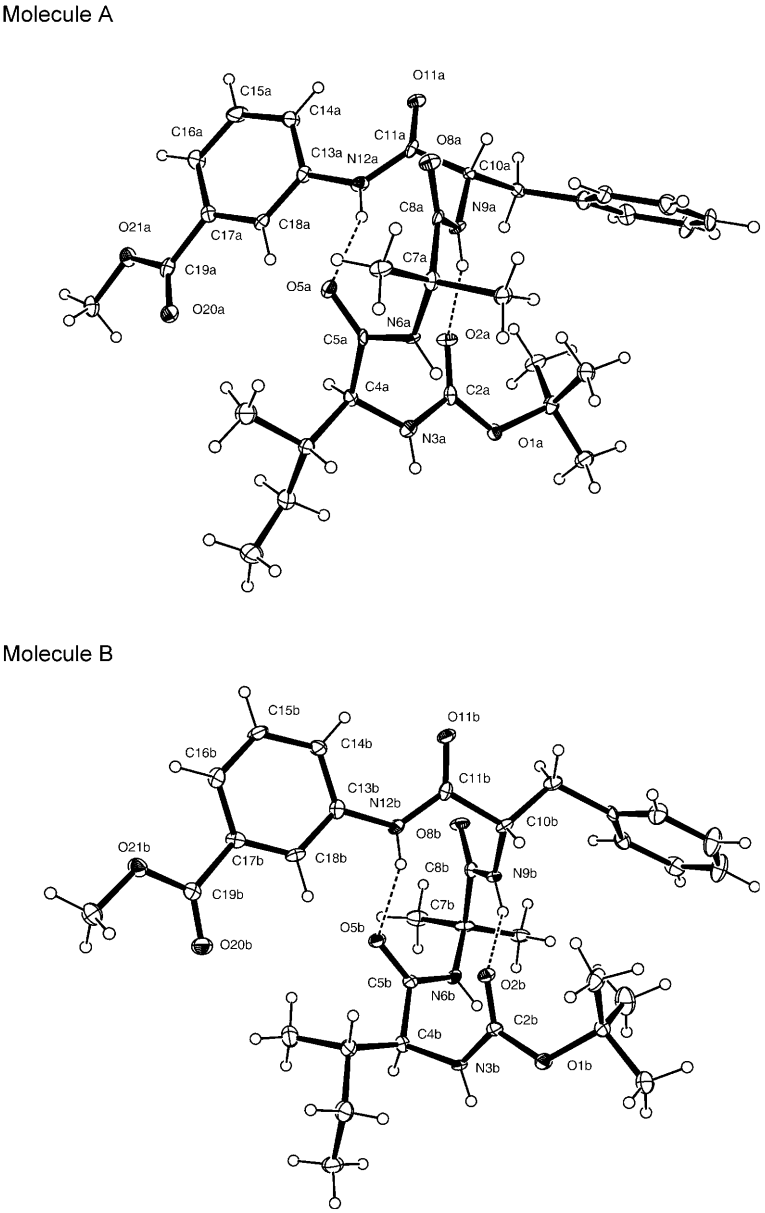

Fig. 3. *ORTEP Diagrams of peptide* **II** *showing molecules A and B both with ellipsoids at 30% probability* (H-bonds shown as dotted lines)

assembly to a supramolecular helix where turns **IIA** and **IIB** are stacked along the *c* axis. For both **A** and **B**, there are two intermolecular H-bonds from NH of Ile(1) to C=O Aib(2), and from NH of Aib(2) to C−O of *m*-ABA(4) in the alternate molecule (*Fig. 5* and *Table 2*). The head-to-tail region meets in good register, so that four strong

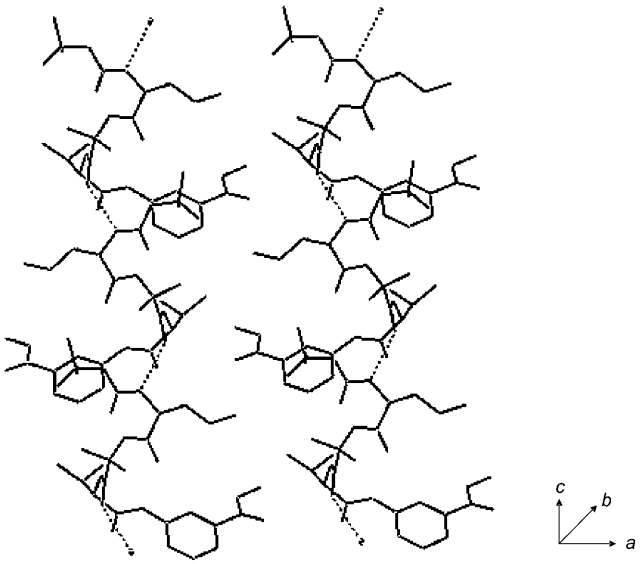

Fig. 4. *The packing of peptide* **I** *showing the intermolecular H-bonded supramolecular helix along the* c *axis.* It also shows the higher-order supramolecular helical assembly. The intermolecular H-bonds are shown as dotted lines.

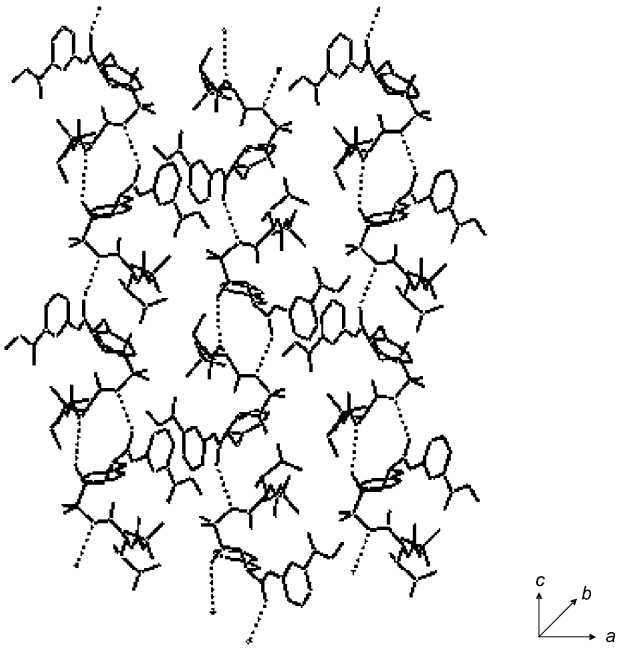

Fig. 5. *The packing of peptide* **II** (A and B) *showing the intermolecular H-bonded supramolecular helix along the* c *axis.* It also shows the higher-order supramolecular helical assembly. The intermolecular H-bonds are shown as dotted lines.

Table 2. *H-Bonding Parameters of Peptides* **I** *and* **II**

D–H···A	H···A [Å]	D···A [Å]	D–H···A [°]
Peptide **I**			
Intramolecular			
N(9)–H(9)···O(2)	2.32	3.173(2)	176
N(12)–H(12)···O(5)	2.12	2.951(2)	164
Intermolecular			
N(3)–H(3)···O(8)[a])	2.15	2.951(2)	156
Peptide **II**			
Intramolecular			
Molecule A			
N(9A)–H(9A)···O(2A)	2.13	2.934(6)	156
N(12A)–H(12A)···O(5A)	2.13	2.946(6)	158
Molecule B			
N(9B)–H(9B)···O(2B)	2.09	2.817(6)	142
N(12B)–H(12B)···O(5B)	2.14	2.930(6)	152
Intermolecular			
N(3A)–H(3A)···O(8B)	2.26	3.116(6)	176
N(6A)–H(6A)···O(11B)	2.18	2.961(6)	152
N(3B)–H(3B)···O(8A)[b])	2.16	2.983(6)	162
N(6B)–H(6B)···O(11A)[b])	2.13	2.950(6)	161

Symmetry elements: [a]) $2-x, y-1/2, 1/2-z$. [b]) $x, y, 1+z$

independent intermolecular H-bonds are formed. The most interesting feature is that two 'diastereoisomeric' turns, **IIA** and **IIB**, of opposite handedness are stacked alternately along the helix axis. As a result, a perpetual reversal of handedness is observed (*Fig. 5*). It is interesting that the structure as a whole fits to 89% of a centrosymmetric structure broken significantly only by the three asymmetric C-atoms which have the (*S*)-configuration in both molecules.

The parallel supramolecular helices of peptides **I** and **II** are further self-assembled through *Van der Waals* interactions (*Figs. 4* and *5*). Interestingly, in the case of peptide **II** the self-assembly is further assisted by the aromatic $\pi-\pi$ interactions between two phenyl rings of *m*-ABAs (*Fig. 5*).

Peptide Conformations in Solution Phase. To investigate the existence of intramolecular H-bonding and peptide conformations in the solution phase, the solvent dependence of the NH chemical shifts were examined by NMR titrations [36]. In this experiment, a solution of peptide **I** in non-polar $CDCl_3$ (10 mM in 0.5 ml) was gradually titrated against polar (D_6)DMSO. The changes in the chemical shifts are presented in *Fig. 6*. The solvent titration shows that, by increasing the percentage of (D_6)DMSO in $CDCl_3$ from 0 to 6.7% (*v*/*v*), the net changes in the chemical-shift ($\Delta\delta$) values for NH H-atoms of Ile(1), Aib(2), Val(3), and *m*-ABA(4) were 0.77, 0.71, 0.05, and 0.20 ppm, respectively (*Fig. 6*). The order of solvent exposure of the NH groups is Ile(1) > Aib(2) > *m*-ABA(4) > Val(3). The $\Delta\delta$ values demonstrate that NH groups of both Val(3) and *m*-ABA(4) are solvent-shielded, and the other two NH groups are solvent-exposed. The result corresponds to a consecutive double β-turn in which the NH groups of Val(3) and *m*-ABA(4) form intramolecular H-bonds as is observed in the crystal

structure (*Fig. 2*). In a similar experiment with peptide **II**, the net changes in the chemical-shift ($\Delta\delta$) values for the NH H-atoms of Ile(1), Aib(2), Phe(3), and *m*-ABA(4) were 0.81, 0.68, 0.19, and 0.18 ppm, respectively (*Fig. 7*). The $\Delta\delta$ values imply that the NH groups of Phe(3) and *m*-ABA(4) are solvent-shielded, and those of Ile(1) and Aib(2) are solvent-exposed, indicating a conformation similar to the crystal structure (*Fig. 3*). The conformations of peptides **I** and **II** were probed further in solution phase by far-UV/CD measurement in MeOH. The CD pattern of peptides **I** and **II** is presented in *Fig. 8*. The anomalous behavior of the CD pattern may be attributed to the presence of *m*-ABA, which can contribute to the CD with its aromatic chromophore. Indeed, such anomalous CD patterns are observed for *m*-ABA-containing peptides [37][38]. The self-aggregation of peptides in MeOH may also cause some changes in the CD pattern.

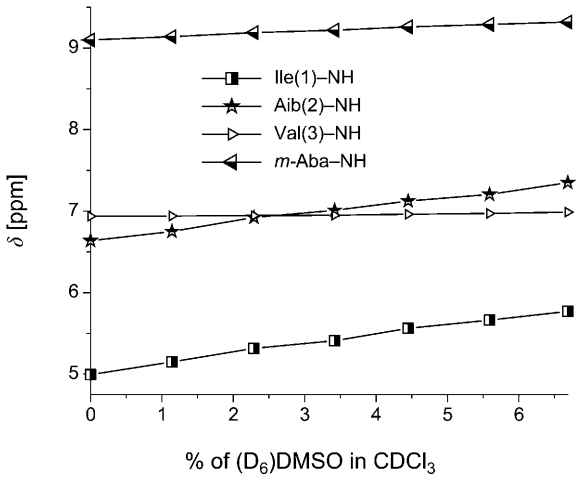

Fig. 6. *NMR Solvent titration curve for NH H-atoms in peptide* **I** (initial concentration of **I**, 10 mM in 0.5 ml $CDCl_3$)

Morphological Studies. Field emission scanning electron-microscopic (FE-SEM) images of the dried fibrous material of the peptides grown slowly from $CHCl_3$/petroleum ether showed that the aggregates in the solid state are bunches of amyloid-like fibrils (*Figs. 9,a*, and *Fig. 10,a*). The high-resolution TEM images also showed the formation of amyloid-like fibrils in the solid state (*Figs. 9,b*, and *Fig. 10,b*). The morphological resemblance of these peptide fibrils with amyloid plaque was also studied by Congo-red staining [15]. Under the cross-polarizer, Congo red-bound fibrils of peptides **I** and **II** exhibited green gold birefringence (*Fig. 11*). These results are consistent with Congo-red binding to an amyloid fibrillar structures. The hierarchical self-assembly of the preorganized double-turn building blocks of peptides **I** and **II** leads to the formation of supramolecular helices which on further aggregation through non-covalent interactions (*Figs. 4* and *5*) produce amyloid-like fibrils.

Conclusions. – The self-assembly of peptides **I** and **II**, occurring through H-bonds between peptide linkages of adjacent molecules, results in the formation of supra-

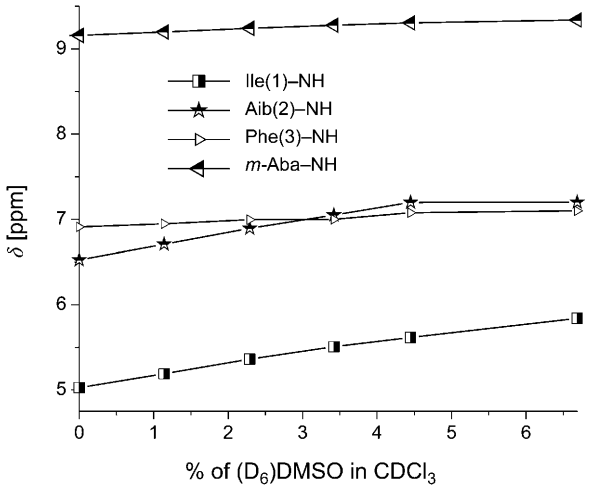

Fig. 7. *NMR Solvent titration curve for NH H-atoms in peptide* **II** (initial concentration of **II**, 10 mM in 0.5 ml $CDCl_3$)

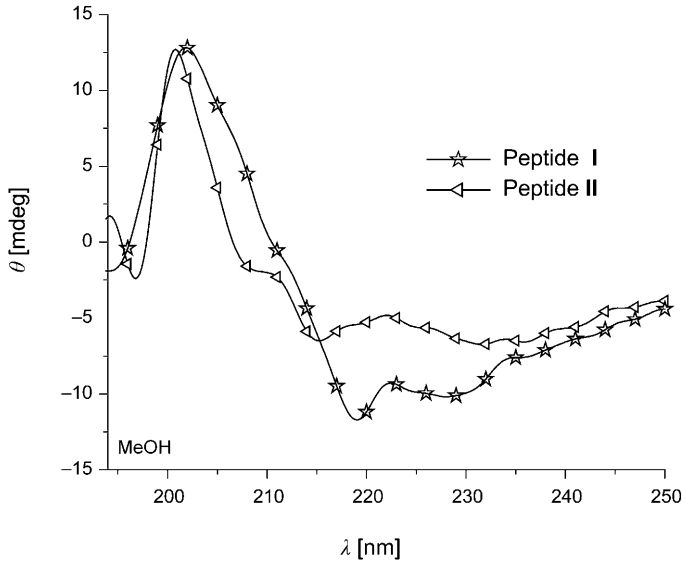

Fig. 8. *CD Curves of peptides* **I** *and* **II** *in MeOH* (1.5 mM)

molecular helical architecture. The hierarchical self-assembly of peptides **I** and **II** leads to amyloid-like fibril formation in the solid state, indicating the mimicry of many naturally occurring macromolecules. In the case of peptide **II**, the supramolecular helix-mediated self-assembly is assisted by the aromatic $\pi-\pi$ interactions between phenyl rings of *m*-ABAs. The atomic model of peptides **I** and **II** significantly increases our understanding of amyloid fibrillogenesis through helix-mediated self-assembly. The

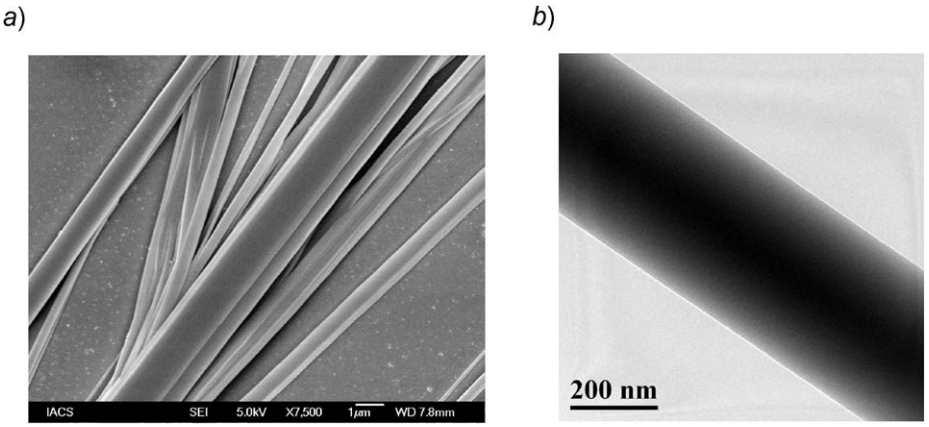

Fig. 9. a) *Field emission scanning electron microscopic* (FE-SEM) *and* b) *high resolution transmission electron-microscopic* (HR-TEM) *images of peptide* **I** *showing the formation of amyloid-like fibrils*

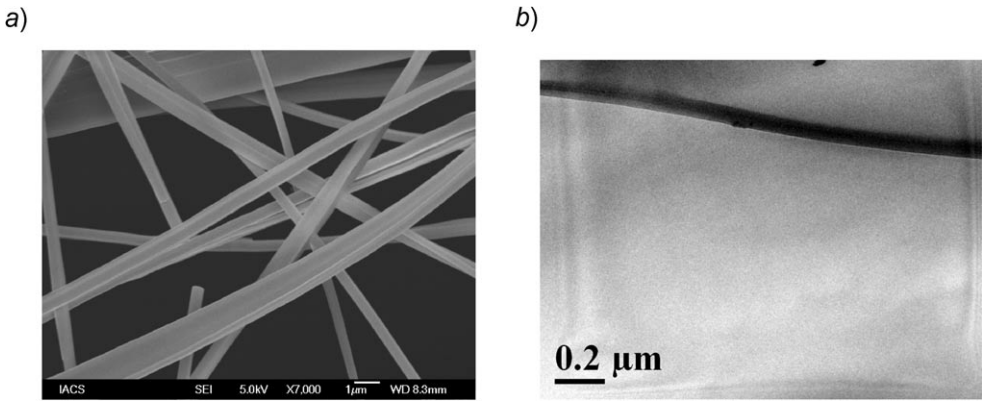

Fig. 10. a) *Field emission scanning electron-microscopic* (FE-SEM) *and* b) *high resolution transmission electron-microscopic* (HR-TEM) *images of peptide* **II** *showing the formation of amyloid-like fibrils*

investigation of the pathway(s) and supramolecular aggregates of amyloid fibril formation have a major role in therapeutics of the amyloid diseases.

A. D. would like to thank *CSIR*, New Delhi, India, for a senior research fellowship (SRF). The financial assistance of *UGC*, New Delhi, is acknowledged (Major Research Project, No. 32-190/2006(SR)). We acknowledge the financial support of *Center for Research in Nanoscience & Nanotechnology*, University of Calcutta. We thank *EPSRC* and the University of Reading, UK, for funds for *Oxford Diffraction X-Calibur CCD* diffractometer.

Experimental Part

General Procedure for the Peptide Synthesis. Peptides **I** and **II** were synthesized by conventional solution-phase methodology [39]. Couplings were mediated by using dicyclohexylcarbodiimide/1-

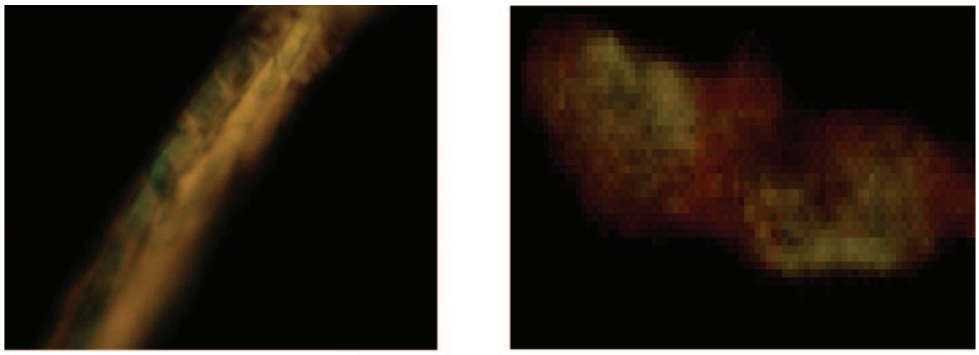

Fig. 11. *The Congo red-stained fibrils of peptides* **I** *and* **II** *observed between crossed polarizers showing green-gold birefringence, a characteristic of amyloid fibrils*

hydroxybenzotriazole (DCC/HOBt). Methyl ester hydrochlorides of peptides were prepared by the $SOCl_2$/MeOH procedure. Methyl ester deprotection was performed *via* saponification. All intermediates were characterized by TLC on silica gel (SiO_2) and used without further purification. Final peptides were purified by column chromatography (CC) using SiO_2 (100–200 mesh) as the stationary phase and an AcOEt/petroleum ether (PE) mixture as the eluent. The reported peptides **I** and **II** were fully characterized by X-ray crystallography, and NMR and IR spectroscopy. Circular dichroism (CD) Spectra: *JASCO* spectropolarimeter (*J-720* model); solns. of peptides **I** and **II** in MeOH (1.5 mM as final concentration). Far-UV/CD: *JASCO* spectropolarimeter (*J-720* model) equipped with a 0.1-cm path length cuvette at 25° with a 0.5-s averaging time, a scan speed of 50 nm/min. The measurements were conducted at 0.2-nm wavelength intervals, 2.0-nm spectral band width and five sequential scans were recorded for each sample. FT-IR Spectra: *Perkin-Elmer-782* model spectrophotometer using the KBr disk technique; $\tilde{\nu}$ in cm^{-1}. ^1H- and ^{13}C-NMR spectra: *Bruker Avance 300* model spectrometer at 300 and 75 MHz, resp.; δ in ppm rel. to Me_4Si as internal standard, J in Hz. The peptide concentrations were 10 mM in $CDCl_3$ for ^1H-NMR and 40 mM in $CDCl_3$ for ^{13}C-NMR. MS: *HEWLETT PACKARD Series 1100MSD* and *Micromass Qtof Micro YA263* mass spectrometers by positive-mode electrospray ionization; in *m*/*z* (rel. %).

Field Emission Scanning Electron Microscopy (FE-SEM). The morphologies of the fibrous materials of peptides **I** and **II** were investigated by FE-SEM. For the FE-SEM study, fibrous materials of the peptides (grown slowly from $CHCl_3$/PE) were dried and Pt-coated. The micrographs were taken in a FE-SEM apparatus (*JEOL JSM-6700F*).

High-Resolution Transmission Electron Microscopy (HR-TEM). The morphology of the reported peptides **I** and **II** were investigated by HR-TEM. A soln. of peptide (1 mg in 1 ml of $CHCl_3$/PE 1:1) was incubated at r.t. overnight. TEM Studies of the peptides were conducted using a small amount of the soln. of the corresponding compounds on carbon-coated Cu grid (300 mesh) by slow evaporation and drying in vaccum at r.t. for 1 d. Images were taken by *JEOL JEM-2100*.

Synthesis of Boc-Ile-Aib-Val-m-*ABA-OMe* (**I**). Initially, the fragment peptide Boc-Ile-Aib-Val-OMe was prepared according to the method described in [40]. Then, the peptide Boc-Ile-Aib-Val-OMe (1.4 g, 3.16 mmol) was dissolved in MeOH (15 ml), and 2M NaOH (5 ml) was added. The mixture was stirred at r.t. for 2 d. The progress of the reaction was monitered by TLC. After completion of the reaction, MeOH was evaporated. The residue obtained was diluted with H_2O and washed with Et_2O. The aq. layer was cooled in ice, neutralized by 2M HCl, and extracted with AcOEt. The solvent was evaporated *in vacuo* to give Boc-Ile-Aib-Val-OH. Yield: 1.3 g (95.8%). White solid. Then, the peptide Boc-Ile-Aib-Val-OH (1.2 g, 2.79 mmol) was dissolved in DMF (5 ml). *m*-ABA-OMe, obtained from its hydrochloride (1.05 g, 5.6 mmol), was added, followed by DCC (0.86 g, 4.2 mmol) and HOBT (0.38 g, 2.79 mmol). The mixture

was stirred at r.t. for 3 d. The precipitated dicyclohexylurea (DCU) was filtered, and to the filtrate AcOEt (20 ml) was added. The org. layer was washed with 1N HCl (3 × 30 ml), 1M Na_2CO_3 soln. (3 × 30 ml), and H_2O. The solvent was then dried (Na_2SO_4) and evaporated *in vacuo* to give **I**. Yield: 1.4 g (91.6%). Light-yellow gum. Purification was performed using SiO_2 as stationary phase and AcOEt/PE as the eluent. Single crystals were grown from $CHCl_3$/PE mixture by slow evaporation. M.p. 178–180°. IR (KBr): 3420, 3302, 1724, 1665, 1604, 1547, 1511. ^{1}H-NMR (300 MHz, $CDCl_3$): 0.92–1.01 (*m*, Me(δ) of Ile, 2 Me(γ) of Val); 1.29–1.27 (*m*, CH_2(γ), Me(γ) of Ile); 1.44 (*s*, 3 Me of Boc); 1.55 (*s*, 2 Me(β) of Aib); 1.95–1.93 (*m*, H–C(β) of Ile); 2.70–2.65 (*m*, H–C(β) of Val); 3.89–3.84 (*m*, H–C(α) of Ile); 3.91 (*s*, MeO); 4.58–4.54 (*m*, H–C(α) of Val); 5.04 (*d*, *J* = 3.9, NH of Ile), 6.68 (*s*, NH of Aib); 6.95 (*d*, *J* = 8.4, NH of Val); 7.36 (*t*, *J* = 8.1, H–C(5) of *m*-ABA); 7.75 (*d*, *J* = 7.8, H–C(4) of *m*-ABA); 8.17 (*d*, *J* = 6.9, H–C(6) of *m*-ABA); 8.49 (*s*, H–C(2) of *m*-ABA)); 9.12 (*s*, NH of *m*-ABA). ^{13}C-NMR (75 MHz; $CDCl_3$): 11.52; 15.74; 16.9; 19.5; 24.0; 25.3; 27.5; 28.1; 29.1; 36.4; 51.9; 57.2; 59.3; 60.7; 81.2; 121.1; 124.5; 124.9; 128.6; 130.5; 138.9; 156.5; 167.1; 170.1; 171.9; 173.9. HR-MS: 571.3107 ($[M + Na]^+$, $C_{28}H_{44}N_4NaO_7^+$; calc. 571.3108). Anal. calc. for $C_{28}H_{44}N_4O_7$ (548.67): C 61.29, H 8.08, N 10.21; found: C 61.21, H 7.95, N 10.08.

*Synthesis of Boc-Ile-Aib-Phe-*m*-ABA-OMe* (**II**). Initially, the fragment peptide Boc-Ile-Aib-Phe-OMe was prepared according to the method described in [40]. Then, the peptide Boc-Ile-Aib-Phe-OMe (1.5 g, 3.14 mmol) was dissolved in MeOH (15 ml), and 2M NaOH (5 ml) was added. The mixture was stirred at r.t. for 2 d. The progress of the reaction was monitered by TLC. After completion of the reaction, MeOH was evaporated. The residue obtained was diluted with H_2O and washed with Et_2O. The aq. layer was cooled in ice, neutralized by 2M HCl, and extracted with AcOEt. The solvent was evaporated *in vacuo* to give Boc-Ile-Aib-Phe-OH. Yield: 1.4 g (96.3%). White solid. Then, the peptide Boc-Ile-Aib-Phe-OH (1.3 g, 2.81 mmol) was dissolved in DMF (5 ml). *m*-ABA-OMe, obtained from its hydrochloride (1.04 g, 5.62 mmol), was added to the above soln., followed by DCC (0.87 g, 4.22 mmol) and HOBT (0.34 g, 2.81 mmol). The mixture was stirred at r.t. for 3 d. The precipitated dicyclohexylurea (DCU) was filtered, and to the filtrate AcOEt (20 ml) was added. The org. layer was washed with 1N HCl (3 × 30 ml), 1M Na_2CO_3 soln. (3 × 30 ml), and H_2O. The resulting soln. was then dried (Na_2SO_4) and evaporated *in vacuo* to give **II**. Yield: 1.5 g (89.6%). Light-yellow gum. Purification was achieved using SiO_2 as stationary phase and AcOEt/PE as the eluent. Single crystals were grown from $CHCl_3$/PE by slow evaporation. M.p. 142–144°. IR (KBr): 3299, 1728, 1667, 1604, 1542, 1452. ^{1}H-NMR (300 MHz, $CDCl_3$): 0.87–0.92 (*m*, Me(δ) of Ile); 1.30–1.19 (*m*, CH_2(γ), Me(γ) of Ile); 1.36 (*s*, 3 Me of Boc); 1.48 (*s*, 2 Me(β) of Aib); 1.86–1.84 (*m*, H–C(β) of Ile); 3.13–3.05 (*m*, CH_2(β) of Phe); 3.82–3.79 (*m*, H–C(α) of Ile); 3.89 (*s*, MeO); 4.91–4.88 (*m*, H–C(α) of Phe); 5.25 (*d*, *J* = 4.2, NH of Ile); 6.76 (*s*, NH of Aib); 7.02 (*d*, *J* = 8.1, NH of Phe); 7.28–7.19 (*m*, 5 arom. H of Ph); 7.37 (*t*, *J* = 8.1, H–C(5) of *m*-ABA); 7.76 (*d*, *J* = 7.8, H–C(4) of *m*-ABA); 8.21 (*d*, *J* = 8.1, H–C(6) of *m*-ABA); 8.54 (*s*, H–C(2) of *m*-ABA); 9.26 (*s*, NH of *m*-ABA). ^{13}C-NMR (75 MHz, $CDCl_3$): 11.3; 15.5; 23.9; 25.3; 26.2; 28.1; 36.4; 36.7; 51.9; 54.5; 56.8; 60.5; 80.9; 121.2; 124.5; 124.9; 126.6; 128.4; 128.6; 128.7; 130.4; 137.5; 138.9; 156.8; 167.0; 169.9; 172.3; 173.6. HR-MS: 619.3104 ($[M + Na]^+$, $C_{32}H_{44}N_4NaO_7^+$; calc. 619.3108). Anal. calc. for $C_{32}H_{44}N_4O_7$ (596.71): C 64.41, H 7.43, N 9.39; found: C 64.27, H 7.31, N 9.28.

Single-Crystal X-Ray Diffraction Study[1]). Details of data collection and refinement are given in *Table 3*. Data were collected with MoK_α radiation using the *Oxford Diffraction X-Calibur CCD System*. The crystals were positioned at 50 mm from the CCD. 321 Frames were measured with a counting time of 10 s. Data analyses were carried out with the CrysAlis program [41]. The structures were solved using direct methods with the SHELXS97 program [42]. The non-H-atoms were refined with anisotropic thermal parameters. The H-atoms bonded to C- and N-atoms were included in geometric positions and given thermal parameters equivalent to 1.2 times those of the atom to which they were attached. The structure of peptide **II** was twinned in a merohedral fashion (*hkl*, *hk* – l) with a refined ratio of 0.56(1):0.44(1). Peptide **II** contained two independent molecules, one of which showed disorder in the position of a Me group. The structure superficially fits to spacegroup $P2_1/c$, but we were unable to obtain

---

[1]) CCDC-724669 and -724670 contain the supplementary crystallographic data for peptides **I** and **II**, resp. These data can be obtained free of charge from the *Cambridge Crystallographic Data Centre*, 12 Union Road, Cambridge CB21EZ, UK; fax: +44-1223-336033; e-mail: deposit@ccdc.cam.ac.uk.

an R_1 value lower than 0.185 with wR_2 0.411, and so space group $P2_1$ with two independent molecules was considered to be correct. Both structures were refined on F^2 using SHELXS97 [42].

Table 3. *Crystallographic Data of Peptides* **I** *and* **II**

	I	**II**
Crystallized from	$CHCl_3$/PE	$CHCl_3$/PE
Formula	$C_{28}H_{44}N_4O_7$	$C_{32}H_{44}N_4O_7$
Formula weight [g mol^{-1}]	548.67	596.71
Crystal dimensions [mm]	$0.30 \times 0.03 \times 0.03$	$0.22 \times 0.03 \times 0.02$
Crystal color	Colorless	Colorless
Temp. [*K*]	150(2)	150(2)
Crystal system	Orthorhombic	Monoclinic
Space group	$P2_12_12_1$	$P2_1$
Z	4	4
Unit cell parameters:		
a [Å]	11.2918(4)	11.4403(7)
b [Å]	15.7846(5)	17.0058(11)
c [Å]	16.6448(6)	16.2704(12)
β [°]	90	90.154(5)
V [Å^3]	2966.71(18)	3165.4(4)
$D_{calc.}$ [g cm^{-3}]	1.228	1.252
R_{int}	0.0207	0.0783
Number of independent reflections	8408	14097
Reflections with $I > 2\sigma(I)$	7073	9731
$R_1(I > 2\sigma(I))$	0.0441	0.0748
wR_2 $(I > 2\sigma(I))$	0.0970	0.1510

Congo Red-Binding Assay. The peptide fibrils generated from **I** and **II** were stained by the addition of alkaline Congo red soln. (80% MeOH/ 20% glass dist. H_2O containing 10 µl of 1% NaOH) for 2 min, and then excess stain was removed by rinsing the stained fibrils with glass dist. H_2O for several times. The stained fibrils were dried under vacuum at r.t. for 24 h, then visualized at 40× magnification, and birefringence was observed between crossed polarizer.

REFERENCES

[1] G. N. Ramachandran, G. Kartha, *Nature* **1955**, *176*, 593.
[2] R. E. Franklin, *Nature* **1955**, *175*, 379.
[3] M. Crisma, C. Toniolo, S. Royo, A. I. Jiménez, C. Cativiela, *Org. Lett.* **2006**, *8*, 6091.
[4] D. Haldar, A. Banerjee, M. G. B. Drew, A. K. Das, A. Banerjee, *Chem. Commun*. **2003**, 1406.
[5] T. Arvinte, A. Cudd, A. F. Drake, *J. Biol. Chem.* **1993**, *268*, 6415.
[6] M. Sadqi, F. Hernández, U. Pan, M. Pérez, M. D. Schaeberle, J. Ávila, V. Muñoz, *Biochemistry* **2002**, *41*, 7150.
[7] C. Goldsbury, K. Goldie, J. Pellaud, J. Seelig, P. Frey, S. A. Müller, J. Kistler, G. J. S. Cooper, U. Aebi, *J. Struct. Biol.* **2000**, *130*, 352.
[8] W. Farris, S. Mansourian, Y. Chang, L. Lindsley, E. A. Eckman, M. P. Frosch, C. B. Eckman, R. E. Tanzi, D. J. Selkoe, S. Guénette, *Proc. Natl. Acad. Sci. U.S.A.* **2003**, *100*, 4162.
[9] H. H. Bauer, U. Aebi, M. Häner, R. Hermann, M. Müller, T. Arvinte, H. P. Merkle, *J. Struct. Biol.* **1995**, *115*, 1.
[10] M. Reches, E. Gazit, *Amyloid* **2004**, *11*, 81.
[11] A. Dutt, M. G. B. Drew, A. Pramanik, *Org. Biomol. Chem*. **2005**, *3*, 2250.

[12] S. K. Maji, D. Haldar, M. G. B. Drew, A. Banerjee, A. K. Das, A. Banerjee, *Tetrahedron* **2004**, *60*, 3251.
[13] A. Banerjee, A. K. Das, M. G. B. Drew, A. Banerjee, *Tetrahedron* **2005**, *61*, 5906.
[14] S. Ray, A. K. Das, M. G. B. Drew, A. Banerjee, *Chem. Commun.* **2006**, 4230.
[15] S. Ray, M. G. B. Drew, A. K. Das, A. Banerjee, *Supramol. Chem.* **2006**, *18*, 455.
[16] S. K. Maji, M. G. B. Drew, A. Banerjee, *Chem. Commun.* **2001**, 1946.
[17] H. A. Lashuel, S. R. LaBrenz, L. Woo, L. C. Serpell, J. W. Kelly, *J. Am. Chem. Soc.* **2000**, *122*, 5262.
[18] N. Yamada, K. Ariga, M. Naito, K. Matsubara, E. Koyama, *J. Am. Chem. Soc.* **1998**, *120*, 12192.
[19] J. Naskar, M. G. B. Drew, I. Deb, S. Das, A. Banerjee, *Org. Lett.* **2008**, *10*, 2625.
[20] S. K. Maji, A. Banerjee, M. G. B. Drew, D. Halder, A. Banerjee, *Tetrahedron Lett.* **2002**, *43*, 6759.
[21] A. Banerjee, S. K. Maji, M. G. B. Drew, D. Halder, A. Banerjee, *Tetrahedron Lett.* **2003**, *44*, 699.
[22] C. Toniolo, M. Crisma, F. Formaggio, C. Peggion, *Biopolymers* **2001**, *60*, 396.
[23] J. Venkatraman, S. C. Shankaramma, P. Balaram, *Chem. Rev.* **2001**, *101*, 3131.
[24] I. L. Karle, P. Balaram, *Biochemistry* **1990**, *29*, 6747.
[25] R. Kaul, P. Balaram, *Bioorg. Med. Chem.* **1999**, *7*, 105.
[26] K. A. Brun, A. Linden, H. Heimgartner, *Helv. Chim. Acta* **2008**, *91*, 526.
[27] C. Toniolo, E. Benedetti, *Trends Biochem. Sci.* **1991**, *16*, 350.
[28] R. T. N. Luykx, A. Linden, H. Heimgartner, *Helv. Chim. Acta* **2003**, *86*, 4093.
[29] N. Pradeille, O. Zerbe, K. Möhle, A. Linden, H. Heimgartner, *Chem. Biodiversity* **2005**, *2*, 1127.
[30] J. M. Humphrey, A. R. Chamberlin, *Chem. Rev.* **1997**, *97*, 2243.
[31] E. Gazit, *FASEB J.* **2002**, *16*, 77.
[32] N. Shamala, R. Nagraj, P. Balaram, *J. Chem. Soc., Chem. Commun.* **1978**, 996.
[33] E. Benedetti, A. Bavoso, B. Di Blasio, V. Pavone, C. Pedone, M. Crisma, G. M. Bonora, C. Toniolo, *J. Am. Chem. Soc.* **1982**, *104*, 2437.
[34] V. Pavone, B. di Blasio, A. Santini, E. Benedetti, C. Pedone, C. Toniolo, M. Crisma, *J. Mol. Biol.* **1990**, *214*, 633.
[35] L. K. Nicholson, T. Yamazaki, D. A. Torchia, S. Grzesiek, A. Bax, S. J. Stahl, J. D. Kaufman, P. T. Wingfield, P. Y. S. Lam, P. K. Jadav, C. N. Hodge, P. J. Domaille, C.-H. Chang, *Nat. Struct. Biol.* **1995**, *2*, 274.
[36] I. L. Karle, A. Banerjee, S. Bhattacharjya, P. Balaram, *Biopolymers* **1996**, *38*, 515.
[37] M. H. V. Ramana Rao, S. Kiran Kumar, A. C. Kunwar, *Tetrahedron Lett.* **2003**, *44*, 7369.
[38] G. Srinivasulu, M. H. V. Ramana Rao, S. Kiran Kumar, A. C. Kunwar, *Arkivoc* **2004**, 69.
[39] M. Bodanszky, A. Bodanszky, 'The Practice of Peptide Synthesis', Springer-Verlag, New York, 1984, pp. 1 – 282.
[40] A. Dutt, A. Dutta, R. Mondal, E. C. Spencer, J. A. K. Howard, A. Pramanik, *Tetrahedron* **2007**, *63*, 10282.
[41] CrysAlis, (2006) Oxford Diffraction Ltd., Abingdon, UK.
[42] G. M. Sheldrick, SHELXS97 and SHELXL97, Programs for Crystallographic Solution and Refinement, *Acta Crystallogr., Sect. A* **2008**, *64*, 112.

Received June 8, 2009